Point-Defect-Localized Bound States in the Continuum in Photonic Crystals and Structured Fibers

Sachin Vaidya,[1,*] Wladimir A. Benalcazar,[1] Alexander Cerjan,[1,2,3] and Mikael C. Rechtsman[1]
[1]Department of Physics, The Pennsylvania State University, University Park, Pennsylvania 16802, USA
[2]Sandia National Laboratories, Albuquerque, New Mexico 87123, USA
[3]Center for Integrated Nanotechnologies, Sandia National Laboratories, Albuquerque 87123, New Mexico, USA

(Received 6 February 2021; accepted 7 June 2021; published 9 July 2021)

We show that point defects in two-dimensional photonic crystals can support bound states in the continuum (BICs). The mechanism of confinement is a symmetry mismatch between the defect mode and the Bloch modes of the photonic crystal. These BICs occur in the absence of band gaps and therefore provide an alternative mechanism to confine light. Furthermore, we show that such BICs can propagate in a fiber geometry and exhibit arbitrarily small group velocity which could serve as a platform for enhancing nonlinear effects and light-matter interactions in structured fibers.

DOI: 10.1103/PhysRevLett.127.023605

Over the last three decades, photonic crystals (PhCs) have been shown to exhibit exceptional confinement and transport properties that exploit the existence of a photonic band gap, a band of frequencies where no electromagnetic waves may propagate [1–4]. Photonic band gaps can inhibit spontaneous emission of embedded quantum emitters [5–8], facilitate slow light through band-edge operation [9], or host localized defect modes that can serve as high-Q resonators or waveguides. Confined defect modes form the basis of many devices such as PhC fibers [10,11], spectral filters, and lasers [12,13], and to achieve near-perfect confinement, defect modes are constructed to lie within photonic band gaps so as to spectrally isolate them from the extended states of the PhC. However, this necessitates the use of materials with a sufficiently high refractive index to open complete gaps. An alternative mechanism for confinement could circumvent the need for band gaps, enabling the use of many low-refractive index materials such as glasses and polymers as well as increasing design flexibility for the realization of PhC-based devices.

One possible way to achieve this is by using bound states in the continuum (BICs). BICs are eigenmodes of a system that, despite being degenerate with a continuum of extended states, stay confined; this confinement may result from a variety of mechanisms [14]. For example, modes of a PhC slab that lie above the light line of vacuum and therefore could radiate, can remain perfectly bound to the slab [15–20]. Previous designs with BICs have mostly shown confinement of a mode in one dimension lower than that of the environment. Recently, corner-localized BICs were predicted and observed in two-dimensional chiral-symmetric systems with higher-order topology [21,22]. However, chiral (sublattice) symmetry is, in general, strongly broken in all-dielectric PhCs. Indeed, confinement in the continuum has to this point not yet been achieved in point defects embedded inside multidimensional PhCs.

In this work, we predict the existence of BICs that are exponentially confined to point defects in a two-dimensional PhC environment. The defect cavity and bulk PhC are designed such that radiation leakage is prohibited due to a symmetry mismatch between the defect mode and the ambient continuum states. The BICs proposed here are protected by the simultaneous presence of time-reversal symmetry (TRS) and the point group of the lattice and as such are robust as long as these symmetries are maintained. As an application for these BICs, we also show how they can circumvent band gap requirements and be used as propagating fiber modes with arbitrarily small group velocity in a low-contrast slow-light PhC fiber.

We draw a distinction between our BICs and the previously reported defect modes degenerate with Dirac points in 2D PhCs [23–28]. In the latter case, the confinement of light to a defect site is due to a vanishing density of states at the Dirac point, which is where that confined mode's frequency lies. Characteristically, such defect modes exhibit weak confinement due to the algebraic mode profile away from the defect site. In contrast, the defect modes presented here are bona fide symmetry protected BICs that are exponentially localized to the defect site.

Consider a two-dimensional PhC consisting of a square lattice of disks with dielectric constant ε and radius r embedded in vacuum. This PhC, as shown in Fig. 1(a), is invariant under 90° rotations (C_4, C_4^2, C_4^{-1}), and reflections along the x, y axes and two diagonals (σ_x, σ_y, σ_{d_1}, σ_{d_2}). These symmetry operations constitute the C_{4v} point group. The irreducible Brillouin zone of this lattice contains three inequivalent high symmetry points (HSPs), namely, $\mathbf{\Gamma} = (0,0)$, $\mathbf{X} = (\pi/a, 0)$, and $\mathbf{M} = (\pi/a, \pi/a)$, as shown

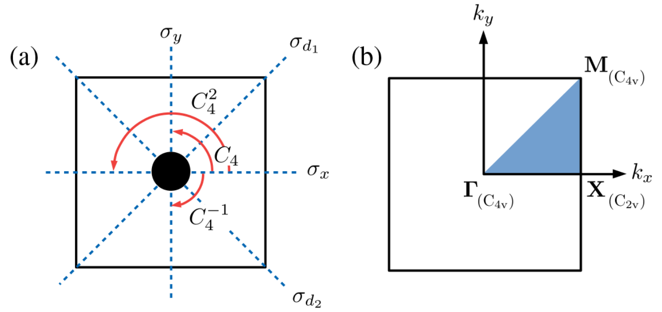

FIG. 1. (a) The unit cell of a two-dimensional PhC consisting of circular disks. The symmetry operators of the C_{4v} point group are labeled. (b) The Brillouin zone of the PhC showing its HSPs and the little groups under which the HSPs are invariant. The solid color consists of all momenta that lie within the irreducible Brillouin zone.

in Fig. 1(b). The HSPs $\mathbf{\Gamma}$ and $\mathbf{M}$ are invariant under the full C_{4v} group, while $\mathbf{X}$ is invariant only under the little group, C_{2v}. Eigenmodes of the PhC at a HSP transform according to the irreducible symmetry representations (irrep) of the group under which the HSP is invariant. The $\mathbf{X}$ point has four possible one-dimensional irreps (a_1, a_2, b_1, b_2) with character table as shown in Table I. Similarly, the $\mathbf{\Gamma}$ and $\mathbf{M}$ points have four one-dimensional irreps (A_1, A_2, B_1, B_2) and one two-dimensional irrep (E) with character table as shown in Table II [2]. The eigenmodes of a C_{4v} symmetric PhC that transform according to the two-dimensional irrep (E) of the C_{4v} point group commonly manifest as quadratic twofold degeneracies at $\mathbf{\Gamma}$ and $\mathbf{M}$ in the presence of TRS. When C_{4v} is broken, this degeneracy splits into two Dirac points as long as inversion and TRS are retained. However, breaking TRS can lift the degeneracy completely [29].

We now describe the general mechanism for creating defect-localized BICs. By changing the geometric parameters of the lattice, the band dispersion of a C_{4v} and TRS-symmetric PhC can be designed such that the twofold degeneracy at either $\mathbf{\Gamma}$ or $\mathbf{M}$ is spectrally isolated from other bands. In a large system consisting of many unit cells of such a PhC (a supercell), a single defect site with radius $r_d \neq r$ is introduced at the center. This creates modes with a significant support on the defect site that generally radiate by hybridizing with the bulk states of the PhC, forming leaky resonances that are characterized by a complex frequency with a negative imaginary part. The frequency of such modes can be tuned by changing the parameters of the defect site such as size or dielectric constant. When the real part of the frequency of the defect mode exactly matches that of the spectrally isolated twofold degeneracy of the bulk, it becomes a perfectly confined BIC provided that the defect mode transforms according to a one-dimensional irrep that is orthogonal to the two-dimensional irrep of the bulk. The presence of this BIC can be inferred from the vanishing of the imaginary part of the frequency and hence a diverging quality factor $Q = -\mathrm{Re}(\omega)/2\mathrm{Im}(\omega)$ of the defect mode.

To demonstrate this, we simulate this system using the finite-difference time domain method (FDTD) as implemented in MEEP [30]. The bulk band requirements are easily met in a simple square lattice of disks with dielectric constant $\varepsilon = 4$ and radius $r/a = 0.275$, where a is the lattice constant in both x and y directions. The chosen values of ε and r/a allow the spectrally isolated twofold degeneracy to occur between TM bands 10 and 11 at the $\mathbf{M}$ point as shown in Fig. 2(a). The photonic density of states (DOS), also shown in the same figure, is given by $\mathrm{DOS}(\omega) = \sum_n \int_{\mathbf{k}\in\mathrm{BZ}} \delta[\omega - \omega_n(\mathbf{k})] d\mathbf{k}$, where $\omega_n(\mathbf{k})$ is the frequency eigenvalue at the momentum $\mathbf{k}$ and band index n. Since each band undergoes an extremum at the degeneracy, the DOS exhibits a jump-discontinuity-type van Hove singularity between two finite and nonzero values. The nonvanishing set of states at the degeneracy forms the continuum within which a BIC can be created.

In a large supercell, we now introduce a defect by changing the radius ($r_d \neq r$) of a single disk in the center of the supercell. As we scan the values of r_d, a BIC emerges for the specific value of the defect radius that corresponds to a mode with the exact frequency of the bulk degeneracy. This is seen from the sharp divergence of the Q factor of the defect mode as shown in Fig. 2(b). Examining the mode profile shown in the inset of Fig. 2(c) reveals that the defect mode transforms according to the irrep A_1, which is prevented from mixing with the basis modes of the orthogonal two-dimensional irrep E of the bulk. Moreover, the mode shows very strong exponential localization to the defect site which can be seen by plotting the intensity envelope as shown in Fig. 2(c). Another important feature of this BIC is its occurrence above $\omega a/2\pi c = 1$. This implies that the lattice constant of the bulk PhC is larger than the wavelength of the BIC mode, a property which

TABLE I. Character table for the C_{2v} point group.

C_{2v}	I	C_2	σ_x	σ_y
a_1	1	1	1	1
a_2	1	1	−1	−1
b_1	1	−1	1	−1
b_2	1	−1	−1	1

TABLE II. Character table for the C_{4v} point group.

C_{4v}	I	$2C_4$	C_2	$2\sigma_{x,y}$	$2\sigma_{d_1,d_2}$
A_1	1	1	1	1	1
A_2	1	1	1	−1	−1
B_1	1	−1	1	1	−1
B_2	1	−1	1	−1	1
E	2	0	−2	0	0

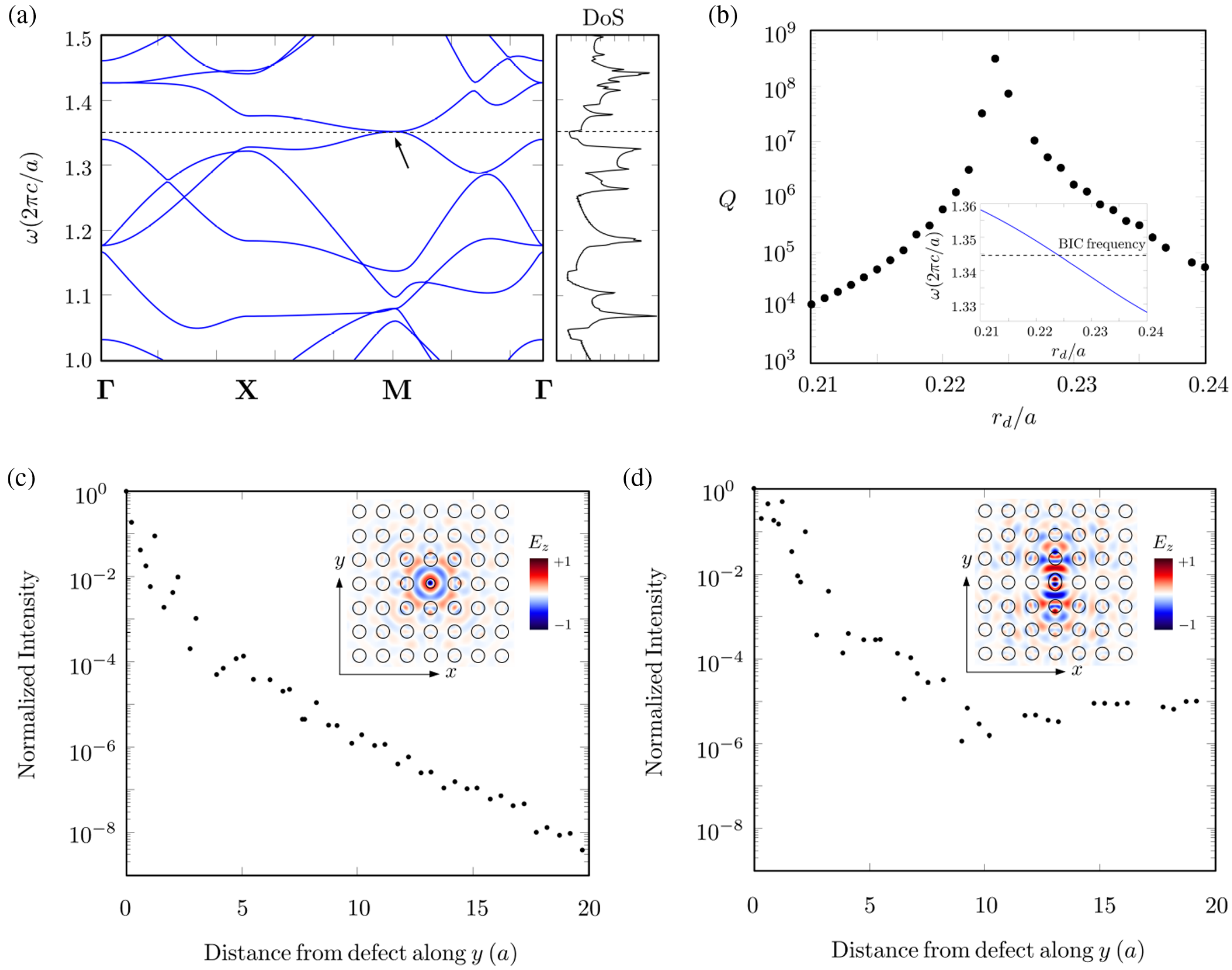

FIG. 2. (a) The TM bands and photonic DOS of a square lattice of dielectric disks of $\varepsilon = 4$ and $r/a = 0.275$ calculated using MIT Photonic Bands (MPB) [31]. The spectrally isolated twofold degeneracy is marked with an arrow. (b) Quality factor (Q) of the defect mode as a function of the defect radius (r_d). The sharp divergence in Q indicates the existence of a BIC at $r_d/a = 0.224$. The inset shows the dependence of the defect mode frequency on r_d. (c) The **E**-field intensity envelope of the BIC showing exponential localization as a function of the distance (along the y axis) from the defect site. The inset shows the z component of the **E** field of the BIC extracted from FDTD simulations. (d) The **E**-field intensity envelope of the resonance when the symmetry of the supercell is reduced from C_{4v} to C_{2v}. The inset shows the z component of the **E** field of the resonance extracted from FDTD simulations.

could prove useful for fabrication because features sizes would need not be subwavelength.

To conclusively show that this BIC is indeed symmetry protected, we change the defect site from a disk to a filled ellipse, which reduces the symmetry of the supercell from C_{4v} to C_{2v}. Because of this deformation, the degeneracy between the two modes that formed the two-dimensional irrep E of C_{4v} is very slightly lifted, and the resultant nondegenerate modes have the one-dimensional irreps b_1 and b_2 of C_{2v}. As before, we vary the defect size to tune the frequency of the defect mode and find a maximum $Q \sim 10^4$ indicating that the mode is not a BIC but a resonance. Indeed, the field pattern of the defect mode as shown in the inset of Fig. 2(d) transforms according to b_2, which coincides with one of the irreps of the bulk enabling the defect and bulk modes to couple and create a leaky resonance with a finite Q (see Supplemental Material [32]). This is also evident from the intensity envelope of the resonance as shown in Fig. 2(d) that markedly demonstrates the lack of exponential confinement to the defect site. Displacing the defect site away from the center also breaks the C_{4v} symmetry of the supercell and has a similar effect of degrading the Q factor of the mode (see Supplemental Material [32]).

The symmetry mismatch between the defect mode and bulk bands requires the existence of a spectrally isolated twofold degeneracy in the bulk PhC, so the question naturally arises: How easy is it to design this bulk band requirement? It is clear from our findings that even simple PhC designs are able to satisfy the requirements for reasonably low dielectric contrast, and in fact, the feature in the TM bands of the PhC discussed in Fig. 2(a) persists

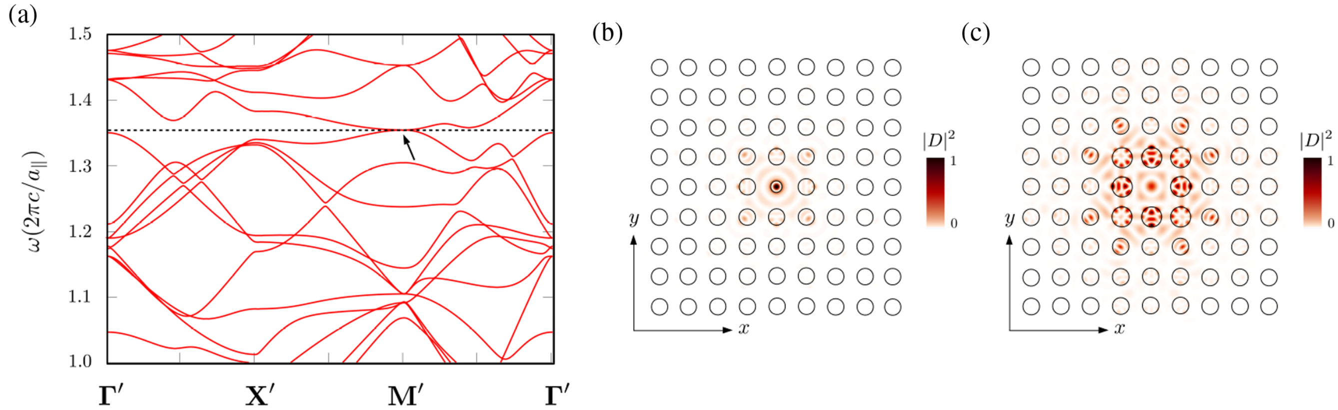

FIG. 3. (a) The $k_\parallel$-band structure of the defect-free PhC fiber at $k_z = 0.18\ (2\pi/a_\parallel)$. The spectrally isolated twofold degeneracy is marked with an arrow. (b) **D**-field intensity profile of a solid-core fiber BIC mode that occurs at $k_z = 0.18\ (2\pi/a_\parallel)$. (c) **D**-field intensity profile of a hollow-core-like fiber BIC mode.

down to $\varepsilon = 3$ for a slightly smaller value of r/a. Furthermore, such quadratic degeneracies can also occur at the $\mathbf{\Gamma}$ point in C_{3v} and C_{6v} symmetric lattices, forming two-dimensional irreps of the respective point groups. In the Supplemental Material [32], we outline a method for finding optimized structures with tunable parameters that exhibit such degeneracies.

For traditional defect modes in 2D PhCs, it suffices to have a band gap for one polarization, either TE or TM, since they constitute orthogonal subspaces that do not mix. However, for applications such as PhC fibers (i.e., where the 2D pattern described above is extruded in the third direction z and $k_z \neq 0$ generally), the distinction between TE and TM is lost, and one requires an overlapping band gap for both polarizations to confine defect modes. In particular, slow-light PhC fibers rely on the existence of a complete band gap at $k_z = 0$, which persists for a small range of k_z [33–35]. The arbitrarily small group velocity of the propagating modes in such fibers is achieved by operating near the $k_z = 0$ band edge. These slowly propagating modes can then be used to strongly enhance interactions of light with either the dielectric material itself or an infiltrated material [36,37], depending on whether the fiber hosts a solid or hollow core. Thus, the design of these fibers requires a high dielectric contrast to open a complete band gap at $k_z = 0$. To the best of our knowledge, the smallest contrast for which a complete band gap exists for 2D PhCs is for $\varepsilon = 4.41$ [38]. We now extend the idea of point-defect-localized BICs to propagating slow-light fiber modes, circumventing the requirement for a complete band gap.

The fiber design that we propose is identical to an extruded version of the 2D PhC discussed before, now consisting of cylinders extended along the direction of propagation in the fiber. However, since the distinction between TE and TM polarizations is lost, the spectrally isolated twofold degeneracy of the bulk must occur in the full band structure in order to create a BIC. This is easily achieved in our structure for a range of k_z values around 0. For instance, Fig. 3(a) shows the band structure of the fiber with $\varepsilon = 4$, $r/a = 0.2755$ at $k_z = 0.18\ (2\pi/a_\parallel)$, where $a_\parallel$ is the lattice constant in the x, y plane. As before, we introduce a defect site and tune the radius r_d and find a BIC at $r_d/a = 0.230$ for this particular value of k_z. The field profile of the BIC is plotted in Fig. 3(b), forming a solid-core mode and displaying strong confinement to the defect site. Since the spectrally isolated twofold degeneracy persists down to $k_z = 0$, the group velocity of this BIC along the length of the fiber $(v_{g_z} = d\omega/dk_z)$ can be made arbitrarily small with an appropriate choice of r_d. It is also possible to create a hollow-core-like fiber mode where the BIC has reasonable support in the air region. To achieve this, we omit the central defect site and instead tune the radius of the nearest eight sites uniformly so as to maintain C_{4v} and find a BIC as shown in Fig. 3(c).

The BICs presented here could be experimentally realized in a variety of systems. For example, these principles could be applied to create high-Q nanocavities in gapless PhC slabs where some vertical leakage is unavoidable but in-plane leakage could be suppressed through the symmetry mismatch mechanism. Functionally, these modes would behave similarly to run-of-the-mill PhC slab-based cavities that rely on a band gap but could be realizable in alternative structures with potentially lower dielectric contrast. Similarly, the PhC fiber design discussed here could be implemented straightforwardly by complex fiber drawing techniques [11]. Furthermore, such isolated degeneracies are also known to occur in 3D PhCs, which could lead to true gapless confinement of light in all directions such as in structures that are precursors to ones with Weyl points [39–42]. Evidently, these BICs rely solely on symmetry considerations and can also be readily realized using other periodic systems such as acoustic crystals, waveguides [22,43], and coupled resonator arrays.

In conclusion, we have proposed BICs that are exponentially localized to defects beyond band gaps in both 2D

PhCs and structured fibers. The PhC slow-light fiber implementation relaxes the need for band gaps at $k_z = 0$ and thus allows for a wider range of materials to be used for their implementation. The results presented here have consequences for the general design of PhC-based devices since the requirement for finding band gaps could potentially be replaced with finding isolated degeneracies at HSPs, which occur more commonly at lower dielectric contrast and at higher frequencies in the band structure. Furthermore, it may be possible to use the BIC mechanism to realize hinge modes in higher-order photonic topological insulators [21,22,44–46] due to their structural similarity with PhC fiber modes.

M. C. R. acknowledges support from the Office of Naval Research Multidisciplinary University Research Initiative Grant No. N00014-20-1-2325 on Robust Photonic Materials with High-Order Topological Protection as well as the Packard Foundation under Fellowship No. 2017-66821 and the Kaufman foundation under Grant No. KA2020-114794. W. A. B. is grateful for the support of the Eberly Postdoctoral Fellowship at the Pennsylvania State University. This work was performed, in part, at the Center for Integrated Nanotechnologies, an Office of Science User Facility operated for the U.S. Department of Energy (DOE) Office of Science. Sandia National Laboratories is a multimission laboratory managed and operated by National Technology and Engineering Solutions of Sandia, LLC, a wholly owned subsidiary of Honeywell International, Inc., for the U.S. DOE's National Nuclear Security Administration under Contract No. DE-NA-0003525. The views expressed in the article do not necessarily represent the views of the U.S. DOE or the United States Government. Computations for this research were performed on the Pennsylvania State University's Institute for Computational and Data Sciences Roar supercomputer.

[*]sxv221@psu.edu

[1] J. D. Joannopoulos, S. G. Johnson, J. N. Winn, and R. D. Meade, *Photonic Crystals: Molding the Flow of Light*, 2nd ed. (Princeton University Press, Princeton, NJ, 2008).
[2] K. Sakoda, *Optical Properties of Photonic Crystals*, 2nd ed., Springer Series in Optical Sciences Vol. 80 (Springer, New York, 2005).
[3] J. D. Joannopoulos, P. R. Villeneuve, and S. Fan, Nature (London) **386**, 143 (1997).
[4] S. John, Phys. Rev. Lett. **58**, 2486 (1987).
[5] E. Yablonovitch, Phys. Rev. Lett. **58**, 2059 (1987).
[6] S. Noda, M. Fujita, and T. Asano, Nat. Photonics **1**, 449 (2007).
[7] M. Fujita, S. Takahashi, Y. Tanaka, T. Asano, and S. Noda, Science **308**, 1296 (2005).
[8] M. R. Singh, Phys. Rev. A **75**, 033810 (2007).
[9] T. Baba, Nat. Photonics **2**, 465 (2008).
[10] J. C. Knight, Nature (London) **424**, 847 (2003).
[11] P. Russell, Science **299**, 358 (2003).
[12] M. Imada, S. Noda, A. Chutinan, T. Tokuda, M. Murata, and G. Sasaki, Appl. Phys. Lett. **75**, 316 (1999).
[13] Y. Kurosaka, S. Iwahashi, Y. Liang, K. Sakai, E. Miyai, W. Kunishi, D. Ohnishi, and S. Noda, Nat. Photonics **4**, 447 (2010).
[14] C. W. Hsu, B. Zhen, A. D. Stone, J. D. Joannopoulos, and M. Soljačić, Nat. Rev. Mater. **1**, 16048 (2016).
[15] P. S. Pankin, B.-R. Wu, J.-H. Yang, K.-P. Chen, I. V. Timofeev, and A. F. Sadreev, Commun. Phys. **3**, 91 (2020).
[16] A. Taghizadeh and I.-S. Chung, Appl. Phys. Lett. **111**, 031114 (2017).
[17] A. Cerjan, C. W. Hsu, and M. C. Rechtsman, Phys. Rev. Lett. **123**, 023902 (2019).
[18] C. W. Hsu, B. Zhen, J. Lee, S.-L. Chua, S. G. Johnson, J. D. Joannopoulos, and M. Soljačić, Nature (London) **499**, 188 (2013).
[19] J. Lee, B. Zhen, S.-L. Chua, W. Qiu, J. D. Joannopoulos, M. Soljačić, and O. Shapira, Phys. Rev. Lett. **109**, 067401 (2012).
[20] V. Liu, M. Povinelli, and S. Fan, Opt. Express **17**, 21897 (2009).
[21] W. A. Benalcazar and A. Cerjan, Phys. Rev. B **101**, 161116 (R) (2020).
[22] A. Cerjan, M. Jürgensen, W. A. Benalcazar, S. Mukherjee, and M. C. Rechtsman, Phys. Rev. Lett. **125**, 213901 (2020).
[23] K. Xie, H. Jiang, A. D. Boardman, Y. Liu, Z. Wu, M. Xie, P. Jiang, Q. Xu, M. Yu, and L. E. Davis, Laser Photonics Rev. **8**, 583 (2014).
[24] Q. Mao, K. Xie, L. Hu, Q. Li, W. Zhang, H. Jiang, Z. Hu, and E. Wang, Appl. Opt. **55**, B139 (2016).
[25] Q. Mao, K. Xie, L. Hu, Q. Li, W. Zhang, H. Jiang, Z. Hu, and E. Wang, Opt. Commun. **384**, 11 (2017).
[26] L. Hu, K. Xie, Z. Hu, Q. Mao, J. Xia, H. Jiang, J. Zhang, J. Wen, and J. Chen, Opt. Express **26**, 8213 (2018).
[27] L. Yang, G. Qian, G. Tang, F. Yuan, Z. Zhang, K. Huang, Z. Shi, Q. Qian, and Z. Yang, Opt. Mater. **89**, 203 (2019).
[28] K. Xie, W. Zhang, A. D. Boardman, H. Jiang, Z. Hu, Y. Liu, M. Xie, Q. Mao, L. Hu, Q. Li, T. Yang, F. Wen, and E. Wang, Light **4**, e304 (2015).
[29] Y. D. Chong, X.-G. Wen, and M. Soljačić, Phys. Rev. B **77**, 235125 (2008).
[30] A. F. Oskooi, D. Roundy, M. Ibanescu, P. Bermel, J. Joannopoulos, and S. G. Johnson, Comput. Phys. Commun. **181**, 687 (2010).
[31] S. G. Johnson and J. D. Joannopoulos, Opt. Express **8**, 173 (2001).
[32] See Supplemental Material at http://link.aps.org/supplemental/10.1103/PhysRevLett.127.023605 for simulations of C_{4v} broken supercells, a method for finding spectrally isolated twofold degeneracies using MPB and supercell band structures for identifying defect modes.
[33] J. Grgić, S. Xiao, J. Mørk, A.-P. Jauho, and N. A. Mortensen, Opt. Express **18**, 14270 (2010).
[34] J. Lægsgaard, J. Opt. Soc. Am. B **28**, 37 (2011).
[35] A. F. Oskooi, J. D. Joannopoulos, and S. G. Johnson, Opt. Express **17**, 10082 (2009).
[36] P. S. Donvalkar, S. Ramelow, S. Clemmen, and A. L. Gaeta, Opt. Lett. **40**, 5379 (2015).

[37] J. R. Sparks, J. L. Esbenshade, R. He, N. Healy, T. D. Day, D. W. Keefer, P. J. A. Sazio, A. C. Peacock, and J. V. Badding, J. Lightwave Technol. **29**, 2005 (2011).
[38] A. Cerjan and S. Fan, Phys. Rev. A **96**, 051802(R) (2017).
[39] L. Lu, L. Fu, J. D. Joannopoulos, and M. Soljačić, Nat. Photonics **7**, 294 (2013).
[40] L. Wang, S.-K. Jian, and H. Yao, Phys. Rev. A **93**, 061801 (R) (2016).
[41] Z. Yang, M. Xiao, F. Gao, L. Lu, Y. Chong, and B. Zhang, Opt. Express **25**, 15772 (2017).
[42] S. Vaidya, J. Noh, A. Cerjan, C. Jörg, G. von Freymann, and M. C. Rechtsman, Phys. Rev. Lett. **125**, 253902 (2020).
[43] Y. Plotnik, O. Peleg, F. Dreisow, M. Heinrich, S. Nolte, A. Szameit, and M. Segev, Phys. Rev. Lett. **107**, 183901 (2011).
[44] J. Noh, W. A. Benalcazar, S. Huang, M. J. Collins, K. P. Chen, T. L. Hughes, and M. C. Rechtsman, Nat. Photonics **12**, 408 (2018).
[45] C. W. Peterson, W. A. Benalcazar, T. L. Hughes, and G. Bahl, Nature (London) **555**, 346 (2018).
[46] W. A. Benalcazar, B. A. Bernevig, and T. L. Hughes, Science **357**, 61 (2017).